J Digit Imaging
DOI 10.1007/s10278-017-0020-4

Differences Between Schizophrenic and Normal Subjects Using Network Properties from fMRI

Youngoh Bae[1] · **Kunaraj Kumarasamy**[2] · **Issa M. Ali**[2] · **Panagiotis Korfiatis**[2] · **Zeynettin Akkus**[2] · **Bradley J. Erickson**[2]

Abstract Schizophrenia has been proposed to result from impairment of functional connectivity. We aimed to use machine learning to distinguish schizophrenic subjects from normal controls using a publicly available functional MRI (fMRI) data set. Global and local parameters of functional connectivity were extracted for classification. We found decreased global and local network connectivity in subjects with schizophrenia, particularly in the anterior right cingulate cortex, the superior right temporal region, and the inferior left parietal region as compared to healthy subjects. Using support vector machine and 10-fold cross-validation, nine features reached 92.1% prediction accuracy, respectively. Our results suggest that there are significant differences between control and schizophrenic subjects based on regional brain activity detected with fMRI.

Keywords fMRI · Machine learning · Schizophrenia · Network properties

Introduction

Schizophrenia is a common serious mental health condition, affecting 1% of the general population, and is likely underdiagnosed [1]. Long-term unemployment, poverty, and homelessness are associated with schizophrenia, making diagnosis and treatment of patients not only critical but also more difficult [2]. The causes of schizophrenia are not known, but it is associated with environmental and genetic factors [3]. Because there is no objective test for schizophrenia, clinicians can diagnose it only after carefully observing a subject's symptoms [2], making early diagnosis of schizophrenia difficult. Early diagnosis is important as a distinct improvement in outcome was reported when therapy was instituted early in the course of schizophrenia [4]. An objective method for diagnosis that might allow earlier diagnosis could be valuable.

A growing number of studies have reported the ability to diagnose schizophrenia using imaging techniques such as positron emission tomography (PET), diffusion tensor image (DTI), and fMRI. Numerous PET studies of schizophrenia have been reported by measuring 5-HT2 and dopamine 2 receptor occupancy, and regional cerebral blood flow [5–7]. Most studies of DTI showed white matter abnormalities in schizophrenia [8, 9]. Numerous studies have employed fMRI to focus on understanding psychiatric disease on the basis of brain activation in particular regions or in terms of the relation among regions [9, 10]. Some previous studies have identified abnormalities in subjects with schizophrenia in the regions of brain that show activity during specific tasks [11, 12]. From these imaging data, correlation matrices based on fMRI data were developed [13].

Specific neurological patterns of brain activation have been reported in schizophrenia [14], including the use of graph theory to find the characteristics of psychiatric disorders [15]. Previous research in alcoholism using the combination of global and local parameters based on whole-brain functional networks has been reported [16]. Whole-brain search based on graph theory to compute global and local features, followed by feature reduction to select the best performing features, is the typical process for building a machine learning-based diagnostic tool.

✉ Bradley J. Erickson
bje@Mayo.edu

[1] School of Medicine, CHA University, Seongnam-si, Gyeonggi-do, South Korea

[2] Department of Radiology, Mayo Clinic College of Medicine, Rochester, MN, USA

Published online: 18 September 2017

As MR technology and machine learning techniques advance, a large number of studies have focused on the activation signal in various anatomical regions of the brain [10, 17], and a few of the studies have analyzed functional connectivity among regions of interest [18]. At the same time, a growing number of studies have elucidated psychiatric disorders, in part by using functional connectivity. Examples include attention-deficit/hyperactivity disorder [19], chronic alcoholism [20], Alzheimer's disease [21], bipolar disorder [22], and schizophrenia [23].

Previous studies employ structural MRI, DTI, resting-state fMRI along with machine learning to find patterns that classify schizophrenia versus healthy controls [24–26]. However, classification based on graph theory from working memory task functional image has not been reported. Our purpose was to determine if connectivity of the brain in the subjects with schizophrenia is functionally different from normal subjects.

We describe a machine learning algorithm that uses single-subject fMRI (SS-fMRI) to distinguish schizophrenic subjects from normal controls. We suggest that in addition to assisting with diagnosis, this novel computer-aided method may help researchers to find neurological patterns and understand pathology of the subjects with schizophrenia through graph theory.

Materials and Methods

Subjects

The dataset for this study was acquired by the Conte Center for the Neuroscience of Mental Disorder (CCNMD) at Washington University School of Medicine in St. Louis (https://openfmri.org/dataset/ds000115/ accessed October 20, 2016). This data used is an IRB approved and a publicly available dataset of subjects with schizophrenia and matched controls. Every candidate was diagnosed based on consensus between a research psychiatrist who conducted a semi-structured interview and a trained research assistant who used the Structured Clinical Interview for DSM-IV Axis I Disorders [27]. Candidates were excluded if they (A) had met DSM-IV standards for substance dependence or severe/moderate abuse during the past 6 months, (B) had clinically unstable or severe medical disorders, (C) had a documented history of head injury due to neurological sequelae or loss of consciousness, or (D) met the DSM-IV criteria for mental retardation [28].

Subjects with schizophrenia were outpatients and stabilized with antipsychotic drugs for at least 2 weeks. The control group did not have a history of axis I mental illness or mood disorder. A full description of the controls and subjects is provided in [29].

Original data were composed of 104 candidates (normal subjects = 80, schizophrenic subjects = 24). We excluded 5 subjects because we were not able to download the MRIs, 9 subjects because the demographic data was not complete, and 15 subjects because less than 85 (out of 90 possible) regions of interest (ROIs) were not matched using the automatic data analysis method described below. This number of ROIs was arbitrarily selected because it represents about 96% of data (2 standard deviations). These exclusions were made without knowledge of whether the examination in question was normal or schizophrenic (see Fig. 1 for distribution of exclusions).

Our final dataset consisted of 75 subjects, 21 patients with DSM IV schizophrenia, and 54 healthy control subjects (demographics shown in Table 1). All subjects underwent SS-fMRI during a test of executive function or a working memory problem (0-, 1-, or 2-back accuracy). There was no statistical difference in age (p = 0.17),

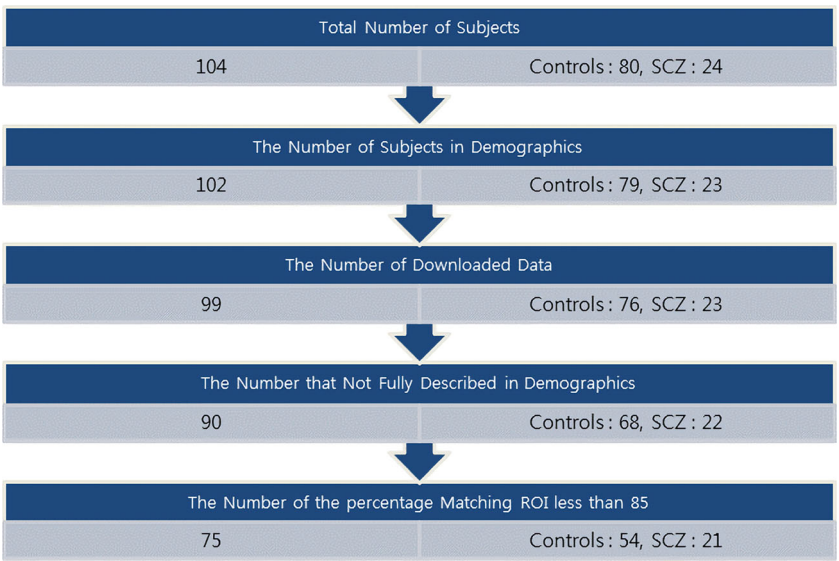

Fig. 1 Exclusions of data. Beginning with 104 subjects, we excluded 5 subjects (4 controls and 1 schizophrenic subjects) because we were unable to download MRI data, 9 subjects (8 controls and 1 schizophrenic subjects) because demographic data was not available, and 15 subjects (14 controls and 1 schizophrenic subjects) because at least 85 ROIs could not be automatically aligned

Table 1 Demographic and clinical leftacteristics and neuropsychological assessment of the schizophrenic and control subjects

Measure	Group[a]		*p* value
	Healthy controls (*N* = 54)	Schizophrenic subjects (*N* = 21)	
Age (years)	22.51 ± 4.49	24.26 ± 3.74	0.17
Sex (% male)	57%	71%	0.33
Subject education (years)	12.98 ± 3.05	12.13 ± 1.87	0.013
Parental education (years)	14.85 ± 2.03	14.6 ± 2.48	0.0.014
Symptom scores[a]			
Positive symptoms	− 0.37 ± 0.31	0.97 ± 1.04	< 0.001
Negative symptoms	− 0.35 ± 0.32	1.00 ± 0.77	< 0.001
Disorganization symptoms	− 0.21 ± 0.29	0.79 ± 0.99	< 0.001
N-back performance			
0-back accuracy	0.96 ± 0.08	0.93 ± 0.15	0.088
1-back accuracy	0.91 ± 0.31	0.85 ± 0.14	< 0.001
2-back accuracy	0.85 ± 0.17	0.74 ± 0.25	< 0.001
Neuropsychological assessment[b]			
IQ	− 0.20 ± 0.32	− 0.87 ± 0.78	0.02
Working memory	0.41 ± 0.38	− 0.43 ± 0.64	< 0.001
Episodic memory	0.29 ± 0.26	− 0.80 ± 0.57	< 0.001
Executive function	0.45 ± 0.13	− 0.32 ± 0.82	< 0.001

Data are given as mean ± SD, except as otherwise indicated

[a] Symptom assessments are described as *Z* scores relative to the mean of whole samples as described [17]

[b] Cognitive assessments are described as *Z* scores relative to the mean of whole samples as described [17]

sex ($p = 0.33$), ethnicity ($p = 0.53$), and scores of *N*-back performance as a test of memory function. However, there were significant differences between groups in terms of level of subject education ($p = 0.013$), parental education ($p = 0.014$), and psychiatric symptom and neuropsychological assessment, though not IQ. One-way ANOVAs indicated significant group differences for positive [$F(1, 59) = 42.56$, $p < 0.001$], negative [$F(1, 59) = 28.22$, $p < 0.001$], and disorganization [$F(1, 59) = 36.24$, $p < 0.001$] symptoms. One-way ANOVAs presented significant group differences for IQ [$F(1, 59) = 11.96$, $p = 0.02$], working memory [$F(1, 59) = 25.07$, $p < 0.001$], episodic memory [$F(1, 59) = 29.73$, $p < 0.001$], and executive function [$F(1, 59) = 17.58$, $p < 0.001$].

MR Scanning

All scans were performed at 3 T on Siemens (Siemens Medical Solutions, Malvern, PA) Tim TRIO scanners at Washington University Medical School. Functional blood oxygen level dependent (BOLD) images using an asymmetric spin-echo, echo planar T2*-weighted sequence (repetition time [TR] = 2500 ms, echo time [TE] = 27 ms, field [FOV] = 256 mm, flip = 90°, voxel size = 4 × 4 × 4 mm). T1 structural images were also acquired using an MP-RAGE 3D sequence (TR = 2400 ms, TE = 3.16 ms, flip = 8°, voxel size = 1 × 1 × 1 mm). A full description of the protocol is provided in [28].

Processing

This processing had three components: feature selection from MR images, classifier training, and evaluation of the ability of the classifier to accurately identify controls versus subjects. Feature selection consisted of preprocessing to obtain useful functional time series data, constructing correlation matrix, calculating network properties using correlation matrix, and conducting feature reduction (Fig. 2).

The functional and structural images were preprocessed as described in [29]. All remaining steps, including realignment, normalization, and coregistration, were performed using statistical parametric mapping [30], which was also used for computing the time series data in each voxel and extracting the mean value of time series data for the ROIs [30]. First, we registered SS-fMRI and structural MR brain images, and the brain portion was masked using statistical parametric mapping (SPM) brain masking toolbox [31]. Second, SPM [30] was used to create anatomic labels for 90 ROIs from the image database.

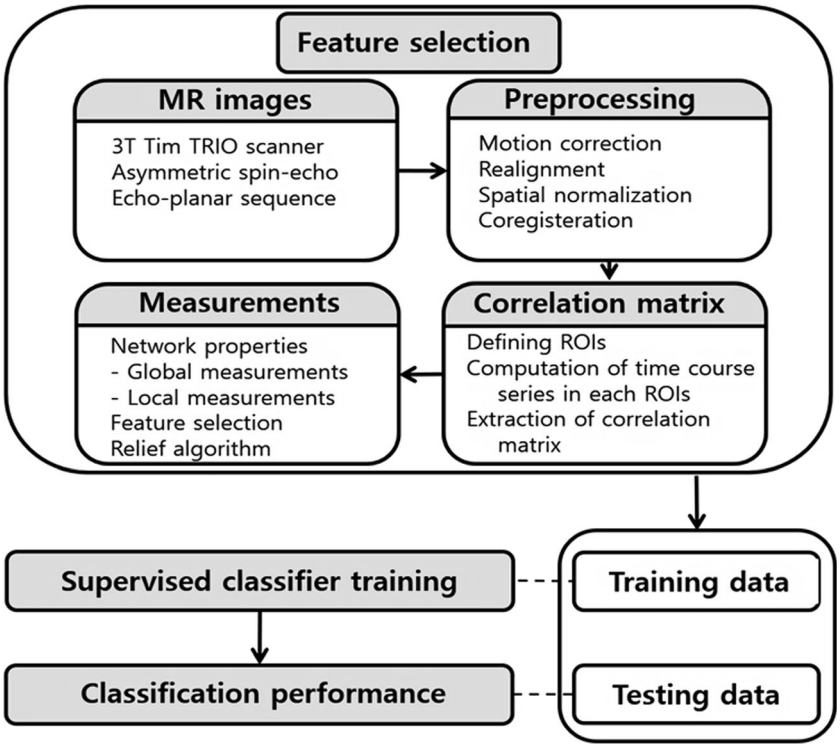

Fig. 2 Schematic design of the proposed system for discriminating between healthy control and schizophrenia groups. This study contained three components: feature selection, classifier training, and testing. *ROIs* regions of interest

Correlation Matrix

To obtain functional connectivity, we constructed a correlation matrix based on the SS-fMRI. To adjust for individual variability and build robust correlation matrix, we used BASCO for automatic selection of 90 ROIs [32], which segments and labels each anatomic region of each subject using the MRI template of SPM and SPM12. We note here that SPM12 provides a major update for this function [30].

To obtain reliable features from network properties, any subject with fewer than 85 ROIs automatically labeled was excluded. For those with at least 85 automatically identified ROIs, any areas that were not automatically labeled were manually labeled such that all had 90 ROIs [33].

Next, change in intensity over time for each of the 90 ROIs was calculated from the average intensity of voxels of the ROI. This time series data was computed for all ROIs for each participant to create a correlation matrix consisting of the Spearman values between the ROIs, indicating ROI–ROI correlation through time. These were computed for the resting time series data, and the calculation was adjusted using the method described in [34]. Spearman correlation was used because it is less sensitive to outliers compared to Pearson correlation [32]. We then converted the correlation values to normalized values using Z transformation to allow for averaging connectivity and statistical testing of the Spearman correlation matrix [32]. We set a threshold of 0.05 for values in this matrix; that is, only values of Spearman correlation significantly greater than the average over all Spearman correlations were considered. Next, weighted normalization of the 8100 elements in this 90 × 90 Spearman correlation matrix was repeatedly performed, and the absolute of any element that had a value greater than 0.5 ($|z\text{-trans}| \sim |r| > 0.5$) was set to 0 to reduce noise and to reduce redundancy while transforming complex data into simpler data. Figure 3 shows the ROIs, intensity data, and the final correlation matrix from one subject.

Computation of Connectivity

Connectivity from the correlation matrix can be computed in several ways, reflecting different types of connectivity. Those used in this study were average neighborhood degree, clustering coefficient, betweenness centrality, degree of connectivity, average connectivity, assortativity, characteristic path length, efficiency, degree to high-ordered system (i.e., clustering coefficient/characteristic path length), transitivity, and strength. In this paper, ROIs from a functional image belong to a node, and their correlations indicate a weighted edge. The definitions of measurements are expressed as follows: degree (K) is the measure of nodes, indicating the number of edges. Average neighborhood degree is an indicator of the average correlation between ROI-ROI for a given node, and its local parameter can be determined as described previously [35]. For a node i,

$$\text{average neighborhood degree} = \left(1 \Big/ s_{-i}\right) \sum_j \hat{I} N(i) w_{ij} k_j,$$

where k_j is the weighted degree of node i, w_{ij} is the weight of the edge that links i and j, and $N(i)$ are the neighbors of node i. The

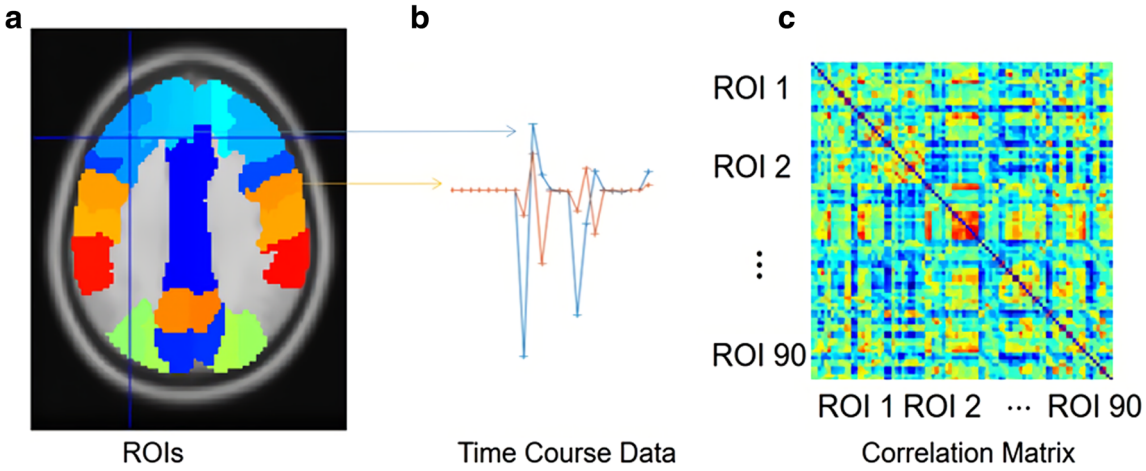

Fig. 3 **a** Anatomic regions of interest (ROIs) produced for 90 anatomical brain regions. All voxels are used in each ROI at each time point to produce. **b** Time series data showing the mean intensity value for two example ROIs through time. **c** Spearman correlation matrix among the time series data of each ROI with all other ROIs for a single subject. The *X-axis* and the *Y-axis* are the labeled ROI for the single subject

global parameters would be the average of neighborhood degrees. Clustering coefficient stands for the ratio of the number of triangles around a node to the number of triangles around a node's neighbors. Its local value can be computed as described previously [36]. For a node i, the

$$\text{clustering coefficient} = \left(1/n\right)\sum_i \hat{I}Nt_i \Big/ \left[\left(k_i^{out}+k_i^{in}\right)\left(k_i^{out}+k_i^{in}-1\right)-2\sum_j \hat{I}Na_{ij}a_{ji}\right],$$

where t_i is the number of triangles around node i, k_i^{out} is the out degree of node i, and k_i^{in} is the in degree of node i. Betweenness centrality in weighted connectivity signifies the degree of participation in all of the shortest paths. This value is calculated as in [36, 37]: For node i,

$$\text{betweenness centrality} = \left[1/(n-1)(n-2)\right]\sum_{h,j}\hat{I}N, h\neq j, h\neq i, j\neq \left[rhj(i)/rhj\right],$$

where r_{hj} is the number of shortest paths between h and j and $r_{hj}(i)$ is the number of shortest paths between h and j that pass through i.

Further description of these features is given elsewhere [38]. Figure 4 graphically illustrates the meaning of network properties. The average neighborhood degree for the yellow node is computed as (1/5)(1 + 2 + 1 + 5 + 2), assuming that weighting is 1. In this expression, each number is written in order of neighbor nodes from left to right. The red node has high betweenness centrality because it would be traversed most frequently if we draw the shortest paths between pairs of nodes. The blue node has a high clustering coefficient value because it has many triangles around, but its neighbors do not. Computation of the above network properties was implemented using the brain connectivity toolbox [38]. Such computations were performed in individual correlation matrices, and their results were used as features.

Feature Reduction

The aim of feature reduction is to identify redundant features and retain only those that have greatest ability to distinguish two classes. Originally, the number of features from the correlation matrix exceeded 1000. Feature reduction is an essential step in machine learning to help avoid spurious associations—if one provides many features, the algorithm can learn specific examples and will not perform well on independent tests nor in the real world. We employed the relief algorithm [39] to select features that were unique and reviewed the importance score. Based on a significant drop between the 9th and 10th scores, we selected the top 9. Independent sample t test was performed on the selected features.

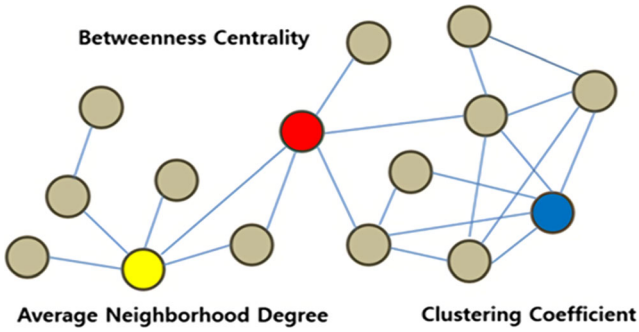

Fig. 4 Graph illustrating the concept of parameters. Nodes depicting average neighborhood degree, betweenness centrality, and clustering coefficient are colored *yellow*, *blue*, and *red*, respectively

Classifier

We applied *K*-nearest neighbor, support vector machine (SVM), decision tree, Naive Bayes, and discriminant analysis (DA) classifiers. We believe that using several classifier methods helps to demonstrate robustness of features—if different machine learning methods produce similar performance, then it is more likely that the features and estimated performance are valid.

An experiment to evaluate the classifier performance using the two sets of features was performed. In this study, five classifiers of significantly different nature were used to help assess generality. First, *K*-nearest neighbor classifier was used for classification. We note here that it was required to compute the Euclidean distance in the multidimensional feature space [40] and was computationally intensive for high-dimensional datasets. The second was SVM, which is known for its high performance, especially for high-dimensional data [41]. Third, a decision tree classifier was used, because its algorithm is an intuitive representation with flow chart-like model of decisions. Although a decision tree classifier is common and easy to understand, it usually performs less well than other classifiers. The fourth classifier was Naive Bayes, a simple probabilistic classifier based on Bayes's theorem [42]. It assumes that each feature is independent of other features and normally distributed, which may not always be true, including in our case. Last, a DA classifier was used to find a linear combination of features that could accurately predict the classes. This classifier also assumes that the features are normally distributed [43].

Cross-Validation Method

For all five classifiers, we applied 10-fold cross-validation to evaluate the robustness of classification performance and assess how well the performance could be generalized to an independent set. The same subject images were used in each of the parameter selection training. In each cross-validation, the data were randomly partitioned into equally sized subsamples with similar ratios of classes. Nine tenths of the data are used for training, and the remaining one tenth is used to test the model. This is repeated 10 times (each time with a different one tenth left out for testing), and the results are averaged to produce a single estimation of classifier performance. This whole procedure repeatedly was conducted 50 times to increase precision of the estimate.

Results

Importance of Features

Figure 5 shows the features with highest importance scores, and Table 2 shows the values and *p* scores for those features in

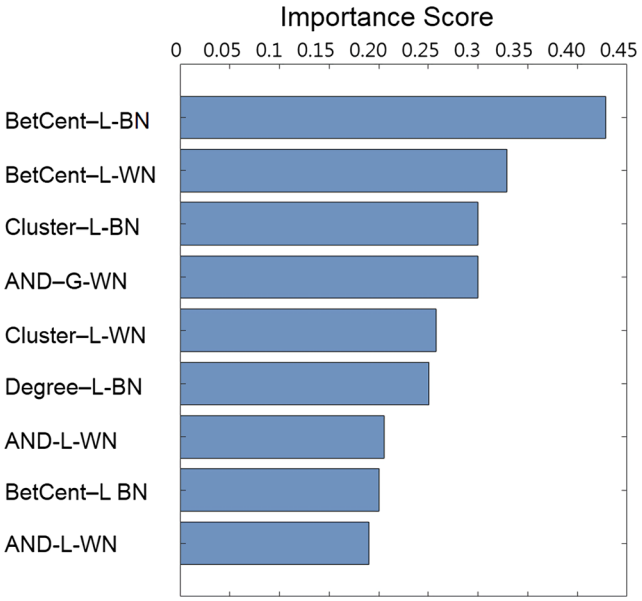

Fig. 5 Results of computing importance scores using relief algorithms. There was a fairly significant drop from feature 1 to feature 2, and again from feature 9 to feature 10

controls and subjects. The highest importance score was computed using the relief algorithm, in which the between centrality in anterior right cingulate cortex was 0.43. The next eight highest importance scores were as follows: the between centrality at the superior right temporal region, the clustering coefficient at the inferior left parietal region, the global average neighborhood degree in the weighted network, the clustering coefficient at the superior right occipital region, the degree parameter at the left olfactory, average neighborhood degree at the inferior orbital right frontal, the between centrality at the superior right frontal, and the average neighborhood degree at the left caudate region. Their values were 0.329, 0.300, 0.258, 0.251, 0.206, 0.200, and 0.190, respectively. For the sake of brevity, effects of all the features are not reported here because their importance scores were lower than those described above.

Feature Differences Between Groups

Table 2 presents the feature measurements for the schizophrenic and control groups. There was a significant difference between the two groups for most of the network properties chosen. The patients with schizophrenia showed lower connectivity except for the between centrality at the anterior right cingulate cortex, the clustering coefficient at the inferior left parietal region, and clustering coefficient at the superior right frontal region.

Performance of Classifier

Table 3 shows the classification accuracy, sensitivity, specificity, and precision of the five classifiers: *K*-nearest

Table 2 The mean (±SD) of functional network properties extracted from the correlation network for healthy controls and the patients with schizophrenia using fMRI signal

Parameter	Regions	Group[a]		p[b]
		Control subjects	Schizophrenic subjects	
BetCent-L-BN	Anterior right cingulate cortex	3.4 ± 1.2	5.2 ± 2.2	< 0.05
BetCent-L-WN	Superior right temporal	62 ± 29	39 ± 18	< 0.01
Cluster-L-BN	Inferior left parietal	0.38 ± 0.07	0.43 ± 0.12	< 0.05
AND-G-WN		0.40 ± 0.07	0.25 ± 0.13	< 0.001
Cluster-L-WN	Superior right occipital	0.34 ± 0.07	0.26 ± 0.12	< 0.001
Degree-L-BN	Left olfactory	61.7 ± 29	38.7 ± 18.6	< 0.01
AND-L-WN	Inferior orbital right frontal	0.43 ± 0.18	0.27 ± 0.19	< 0.005
Cluster-L-BN	Superior right frontal	0.34 ± 0.05	0.39 ± 0.078	< 0.01
AND-L-WN	Left caudate	0.61 ± 0.23	0.34 ± 0.17	< 0.001

BetCent-L-BN between centrality-local-binary network, *BetCent-L-WN* between centrality-local-weighted network, *Cluster-L-BN* clustering coefficient-local-binary network, *AND-G-WN* average neighborhood degree-global-weighted network, *Cluster-L-WN* clustering coefficient-weighted network, *Degree-L-BN* degree-local-binary network, *AND-L-WN* average neighborhood degree-local-weighted network

[a] Data are given as mean ± SD

[b] By independent sample *t* test

neighborhood, SVM, decision tree, Naive Bayes, and DA used for our classification problem using nine features over 50 runs of 10-fold cross-validation. The mean accuracy for *K*-nearest neighborhood classifier is 90.5%, and for the SVM classifier for 10-fold cross-validation, it is 92.1%. While, the accuracy for other methods was somewhat lower, perhaps reflecting the weaker nature of those classifiers. The relatively low standard deviation across the many runs suggests that the results are robust.

Discussion

Our study demonstrated that nine features computed from SS-fMRI can differentiate between schizophrenic and control subjects. Those features were computed using network properties and graph theory techniques. Applying graph theory is novel and potentially useful, given the brain's dynamic network of neuronal connections and statistically significant differences in the networks of healthy and schizophrenic subjects.

Three major differences in the functional connectivity of SS-fMRI were observed between schizophrenic subjects and normal subjects. First, at a global level, as there are some key common properties of network topology reported [44], we found that average neighborhood degree, one of the global features indicating connection between parts of the brain, such as local degree, was significantly reduced in schizophrenia, corroborating earlier results [37]. Second, at a local level, patients showed greater lower value in the between centrality at superior right temporal region to normal subject. At the same time, measured values of schizophrenic patients such as the clustering coefficient in the superior right occipital region, the degree feature in the left olfactory region, and the average neighborhood degree at the inferior orbital right frontal region and the left caudate were lower than that of healthy normal subjects. Conversely, we found that the change in average connectivity, global efficiency, and degree of high ordered system by groups were not significant features. This was also consistent with the previous suggestion that patients with schizophrenia show a shift to reduced functional connectivity of many specific regions, suggesting that brain configuration, as measured by fMRI, is less centralized in schizophrenic subjects [28]. Such results and previous conclusions may support the theory that schizophrenia is a functional disconnectivity syndrome.

Table 3 Mean accuracy, sensitivity, specificity, and precision with standard deviation of each performance after 50 runs of 10-fold cross-validation (each with random partitions) for each classifier

Classifier	Accuracy (%)	Sensitivity (%)	Specificity (%)	Precision (%)
KNN	90.5 ± 6.9	89.1 ± 7.2	93 ± 8.9	93.1 ± 6.3
SVM	92.1 ± 10.5	92.0 ± 15.8	92.1 ± 8.1	94 ± 6.3
Decision tree	82.2 ± 9.4	84.5 ± 17.7	80.7 ± 24.2	88.5 ± 11.1
Naive Bayes	81.0 ± 13.9	89.9 ± 10.2	68.4 ± 24.2	90.9 ± 17.0
DA	88.6 ± 11.4	90 ± 10.5	86.7 ± 18.0	90.2 ± 10.5

SVM support vector machine, *KNN K*-nearest neighborhood, *DA* discriminant analysis

We note here that the subjects in this study were under treatment for their disease, and it is possible that the findings were due to medication, rather than disease. It is not clear what impact medication has on functional connectivity. One might expect that effective medication would reduce the differences from normal controls, but that has not been proven. Our methods may facilitate diagnosis and assessment of schizophrenia, due to their use of structural and functional images. If this is also found to be true for early schizophrenia, it may become an important diagnostic tool and a potential marker of schizophrenia treated.

When focusing on local features, our results from the functional connectivity are consistent with previous studies. Most previous studies have paid attention to abnormal functional features associated with the frontal, temporal, parietal, and occipital regions in schizophrenia [45]. Previous functional neuroimaging studies have demonstrated that abnormal fMRI activation of the anterior cingulate is widely reported in schizophrenia and has been correlated with working memory deficits [46]. Further, neurological research has suggested that there is an abnormal pattern of fronto-temporal interaction in schizophrenia [46]. In addition, frontal–parietal disconnection in schizophrenia had previously been suggested by the deficit in working memory [47]. One recent study implied that as psychosis improved, the left caudate shows decreased functional connectivity [48]. This implication is also consistent with the fact that schizophrenic patients on medication in our study had lower connectivity values with the left caudate.

The support vector machine using nine features showed best accuracy at 92.1%. This compares favorably with other reports using genetic algorithms and SVM based on fMRI data [49]. Despite the high accuracy of our findings, there are several limitations in this study. First, the number of the subjects was rather small. An experiment with a larger population will be needed for generalization. Many subjects had to be removed due to quality issues, and it is striking that most were normal controls. Furthermore, it was assumed that the effect of genetics on functional networks between healthy people and their siblings was insignificant. Some recent studies have found an effect of genetics on functional networks between schizophrenia and their sibling [50]. Third, every schizophrenic subject was taking antipsychotic medication at the time of the diagnostic test. Some of the previous studies suggest that the functional and structural connectivity could be changed as a result of these medications [51]. It is hard to neglect the possibility that medication would not influence on functional connectivity. This study result may be affected by the states of schizophrenic patient and the levels of medications at the same time. Fourth, we used only *N*-back working memory data without resting-state fMRI data. Resting-state fMRI data are expected to yield more reliable results concerning connectivity, as demonstrated in prior studies [52]. Fifth, this study does not consider the types of schizophrenia, but this would be more likely to confound this study than to produce a spurious difference versus normal controls. A larger number of subjects with each form known would be required to assess this problem. Finally, we note that treatment is most effective when schizophrenia is diagnosed early, and the ability of our schema to diagnose early is not known.

Conclusion

We propose a method for classification of normal controls versus schizophrenic subjects based on network properties of whole-brain connectivity from fMRI data. In this study, nine features computed from correlation of brain activity provided high discriminative accuracy across a variety of machine learning methods. The results imply that the brain connectivity in patients with schizophrenia shows properties which are different from those observed in normal controls.

Acknowledgements This work was funded in part by NCI CA160045.

References

1. Wei F, Feng W: Research capacity for mental health in low- and middle-income countries: results of a mapping project. Bull World Health Organ 86:908–908, 2008. https://doi.org/10.2471/blt.08.053249
2. American Psychiatric Association. Diagnostic and Statistical Manual of Mental Disorders (DSM-5®) [Internet]. American Psychiatric Pub; 2013. Available: http://books.google.co.kr/books/about/Diagnostic_and_Statistical_Manual_of_Men.html?hl=&id=-JivBAAAQBAJ
3. Owen MJ, Akira S, Mortensen PB: Schizophrenia. Lancet 388:86–97, 2016. https://doi.org/10.1016/s0140-6736(15)01121-6
4. McGlashan TH, Johannessen JO: Early Detection and Intervention With Schizophrenia: Rationale. Schizophr Bull 22:201–222, 1996. https://doi.org/10.1093/schbul/22.2.201
5. Kapur S, Zipursky RB, Remington G, Jones C, DaSilva J, Wilson AA et al.: 5-HT2 and D2 receptor occupancy of olanzapine in schizophrenia: a PET investigation. Am J Psychiatry 155:921–928, 1998. https://doi.org/10.1176/ajp.155.7.921
6. Friston KJ, Liddle PF, Frith CD, Hirsch SR, Frackowiak RS: The left medial temporal region and schizophrenia. A PET study. Brain 115(Pt 2):367–382, 1992 **A**vailable: https://www.ncbi.nlm.nih.gov/pubmed/1606474
7. Doorduin J, de Vries EFJ, Willemsen ATM, de Groot JC, Dierckx RA, Klein HC: Neuroinflammation in schizophrenia-related psychosis: a PET study. J Nucl Med 50:1801–1807, 2009. https://doi.org/10.2967/jnumed.109.066647
8. Kubicki M, McCarley R, Westin C-F, Park H-J, Maier S, Kikinis R et al.: A review of diffusion tensor imaging studies in schizophrenia. J Psychiatr Res 41:15–30, 2007. https://doi.org/10.1016/j.jpsychires.2005.05.005
9. Schlösser RGM, Nenadic I, Wagner G, Güllmar D, von Consbruch K, Köhler S et al.: White matter abnormalities and brain activation in schizophrenia: a combined DTI and fMRI study. Schizophr Res 89:1–11, 2007. https://doi.org/10.1016/j.schres.2006.09.007

10. Poldrack RA: Region of interest analysis for fMRI. Soc Cogn Affect Neurosci 2:67–70, 2007. https://doi.org/10.1093/scan/nsm006
11. Zhou Y, Yuan Z, Meng L, Tianzi J, Lixia T, Yong L et al.: Functional dysconnectivity of the dorsolateral prefrontal cortex in first-episode schizophrenia using resting-state fMRI. Neurosci Lett 417:297–302, 2007. https://doi.org/10.1016/j.neulet.2007.02.081
12. Welsh RC, Chen AC, Taylor SF: Low-Frequency BOLD Fluctuations Demonstrate Altered Thalamocortical Connectivity in Schizophrenia. Schizophr Bull 36:713–722, 2008. https://doi.org/10.1093/schbul/sbn145
13. Wang Y, Yida W, Cohen JD, Kai L, Turk-Browne NB: Full correlation matrix analysis (FCMA): An unbiased method for task-related functional connectivity. J Neurosci Methods 251:108–119, 2015. https://doi.org/10.1016/j.jneumeth.2015.05.012
14. Frith CD, Friston KJ, Herold S, Silbersweig D, Fletcher P, Cahill C et al.: Regional brain activity in chronic schizophrenic patients during the performance of a verbal fluency task. Br J Psychiatry 167: 343–349, 1995 Available: https://www.ncbi.nlm.nih.gov/pubmed/7496643
15. Shen H, Wang L, Liu Y, Hu D: Discriminative analysis of resting-state functional connectivity patterns of schizophrenia using low dimensional embedding of fMRI. Neuroimage 49:3110–3121, 2010. https://doi.org/10.1016/j.neuroimage.2009.11.011
16. Bae Y, Yoo BW, Lee JC, Kim HC: Automated network analysis to measure brain effective connectivity estimated from EEG data of patients with alcoholism. Physiol Meas 38:759–773, 2017. https://doi.org/10.1088/1361-6579/aa6b4c
17. Lang PJ, Bradley MM, Fitzsimmons JR, Cuthbert BN, Scott JD, Bradley M et al.: Emotional arousal and activation of the visual cortex: An fMRI analysis. Psychophysiology 35:199–210, 1998. https://doi.org/10.1111/1469-8986.3520199
18. Smith SM, Diego V, Beckmann CF, Glasser MF, Mark J, Miller KL et al.: Functional connectomics from resting-state fMRI. Trends Cogn Sci 17:666–682, 2013. https://doi.org/10.1016/j.tics.2013.09.016
19. Bush G, George B, Valera EM, Seidman LJ: Functional Neuroimaging of Attention-Deficit/Hyperactivity Disorder: A Review and Suggested Future Directions. Biol Psychiatry 57: 1273–1284, 2005. https://doi.org/10.1016/j.biopsych.2005.01.034
20. Rogers BP, Parks MH, Nickel MK, Katwal SB, Martin PR: Reduced fronto-cerebellar functional connectivity in chronic alcoholic patients. Alcohol Clin Exp Res 36:294–301, 2012. https://doi.org/10.1111/j.1530-0277.2011.01614.x
21. Allen G, Barnard H, McColl R, Hester AL, Fields JA, Weiner MF et al.: Reduced hippocampal functional connectivity in Alzheimer disease. Arch Neurol 64:1482–1487, 2007. https://doi.org/10.1001/archneur.64.10.1482
22. Chepenik LG, Mariella R, Michelle H, Cheryl L, Fei W, Jones MM et al.: Functional connectivity between ventral prefrontal cortex and amygdala at low frequency in the resting state in bipolar disorder. Psychiatry Research: Neuroimaging 182:207–210, 2010. https://doi.org/10.1016/j.pscychresns.2010.04.002
23. Meyer-Lindenberg A, Poline JB, Kohn PD, Holt JL, Egan MF, Weinberger DR et al.: Evidence for abnormal cortical functional connectivity during working memory in schizophrenia. Am J Psychiatry 158:1809–1817, 2001. https://doi.org/10.1176/appi.ajp.158.11.1809
24. Zarogianni E, Moorhead TWJ, Lawrie SM: Towards the identification of imaging biomarkers in schizophrenia, using multivariate pattern classification at a single-subject level. Neuroimage Clin 3: 279–289, 2013. https://doi.org/10.1016/j.nicl.2013.09.003
25. Zhu M, Jie N, Jiang T: Automatic classification of schizophrenia using resting-state functional language network via an adaptive learning algorithm. SPIE Medical Imaging. Int Soc Optics Photon 903522–903522–6, 2014. doi:https://doi.org/10.1117/12.2043240
26. Arbabshirani MR, Castro E, Calhoun VD: Accurate classification of schizophrenia patients based on novel resting-state fMRI features. 2014 36th Annual International Conference of the IEEE Engineering in Medicine and Biology Society. IEEE, pp 6691–6694. doi:https://doi.org/10.1109/EMBC.2014.6945163
27. First MB, Spitzer RL, Gibbon M, Williams JBW, et al: Structured clinical interview for DSM-IV-TR axis I disorders, research version, patient edition. SCID-I/P, 2002
28. Repovs G, Grega R, Csernansky JG, Barch DM: Brain Network Connectivity in Individuals with Schizophrenia and Their Siblings. Biol Psychiatry 69:967–973, 2011. https://doi.org/10.1016/j.biopsych.2010.11.009
29. Repovš G, Grega R, Barch DM. Working Memory Related Brain Network Connectivity in Individuals with Schizophrenia and Their Siblings. Front Hum Neurosci. 2012;6. doi:https://doi.org/10.3389/fnhum.2012.00137
30. Penny WD, Friston KJ, Ashburner JT, Kiebel SJ, Nichols TE: Statistical Parametric Mapping: The Analysis of Functional Brain Images [Internet]. Academic Press, 2011. Available: http://books.google.co.kr/books/about/Statistical_Parametric_Mapping_The_Analy.html?hl=&id=G_qdEsDlkp0C
31. Ridgway GR, Omar R, Ourselin S, Hill DLG, Warren JD, Fox NC: Issues with threshold masking in voxel-based morphometry of atrophied brains. Neuroimage 44:99–111, 2009. https://doi.org/10.1016/j.neuroimage.2008.08.045
32. Göttlich M, Martin G, Frederike B, Krämer UM: BASCO: a toolbox for task-related functional connectivity. Front Syst Neurosci 9, 2015. https://doi.org/10.3389/fnsys.2015.00126
33. Brett M, Anton J-L, Valabregue R, Poline J-B: Region of interest analysis using the MarsBar toolbox for SPM 99. Neuroimage 16: S497, 2002 Available: http://matthew.dynevor.org/research/abstracts/marsbar/marsbar.pdf
34. Rousselet GA, Pernet CR: Improving standards in brain-behavior correlation analyses. Front Hum Neurosci 6:119, 2012. https://doi.org/10.3389/fnhum.2012.00119
35. Pastor-Satorras R, Romualdo P-S, Alexei V, Alessandro V: Dynamical and Correlation Properties of the Internet. Phys Rev Lett 87, 2001. https://doi.org/10.1103/physrevlett.87.258701
36. Watts DJ, Strogatz SH: Nature 393:440–442, 1998. https://doi.org/10.1038/30918
37. Freeman LC: Centrality in social networks conceptual clarification. Soc Networks 1:215–239, 1978. https://doi.org/10.1016/0378-8733(78)90021-7
38. Rubinov M, Sporns O: Complex network measures of brain connectivity: uses and interpretations. Neuroimage 52:1059–1069, 2010. https://doi.org/10.1016/j.neuroimage.2009.10.003
39. Gao L, Lun G, Taifu L, Lizhong Y, Feng W: Research and application of data mining feature selection based on relief algorithm. J Softw Maint Evol Res Pract 9, 2014. doi:https://doi.org/10.4304/jsw.9.2.515-522
40. Altman NS: An Introduction to Kernel and Nearest-Neighbor Nonparametric Regression. Am Stat 46:175, 1992. https://doi.org/10.2307/2685209
41. Meyer D, David M, Friedrich L, Kurt H: The support vector machine under test. Neurocomputing 55:169–186, 2003. https://doi.org/10.1016/s0925-2312(03)00431-4
42. Surhone LM, Timpledon MT, Marseken SF: Naive Bayes Classifier: Classifier (mathematics), Bayes' Theorem, Probability Theory, Bayesian Inference, Bayesian Probability, Empirical Bayes Method, Statistics, Conditional Probability [Internet]. 2010. Available: http://books.google.co.kr/books/about/Naive_Bayes_Classifier.html?hl=&id=rIAwQwAACAAJ
43. Cover TM: Geometrical and Statistical Properties of Systems of Linear Inequalities with Applications in Pattern Recognition. IEEE Trans Comput EC-14:326–334, 1965. https://doi.org/10.1109/pgec.1965.264137

44. Rubinov M, Knock SA, Stam CJ, Micheloyannis S, Harris AWF, Williams LM, et al: Small-world properties of nonlinear brain activity in schizophrenia. Hum Brain Mapp. Wiley Online Library 30: 403–416, 2009. Available: http://onlinelibrary.wiley.com/doi/10.1002/hbm.20517/full
45. Heckers S, Goff D, Weiss AP: Reversed hemispheric asymmetry during simple visual perception in schizophrenia. Psychiatry Res 116:25–32, 2002 Available: https://www.ncbi.nlm.nih.gov/pubmed/12426031
46. Fletcher P, McKenna PJ, Friston KJ, Frith CD, Dolan RJ: Abnormal cingulate modulation of fronto-temporal connectivity in schizophrenia. Neuroimage 9:337–342, 1999. https://doi.org/10.1006/nimg.1998.0411
47. Kim J-J, Kwon JS, Park HJ, Youn T, Kang DH, Kim MS et al.: Functional disconnection between the prefrontal and parietal cortices during working memory processing in schizophrenia: a [15O] H2O PET study. Am J Psychiatry. Am Psychiatric Assoc 160:919–923, 2003 Available: http://ajp.psychiatryonline.org/doi/abs/10.1176/appi.ajp.160.5.919
48. Sarpal DK, Robinson DG, Lencz T, Argyelan M, Ikuta T, Karlsgodt K et al.: Antipsychotic treatment and functional connectivity of the striatum in first-episode schizophrenia. JAMA Psychiatry 72:5–13, 2015. https://doi.org/10.1001/jamapsychiatry.2014.1734
49. Yang H, Liu J, Sui J, Pearlson G, Calhoun VD: A Hybrid Machine Learning Method for Fusing fMRI and Genetic Data: Combining both Improves Classification of Schizophrenia. Front Hum Neurosci 4:192, 2010. https://doi.org/10.3389/fnhum.2010.00192
50. Wang Q, Cheng W, Li M, Ren H, Hu X, Deng W et al.: The CHRM3 gene is implicated in abnormal thalamo-orbital frontal cortex functional connectivity in first-episode treatment-naive patients with schizophrenia. Psychol Med 46:1523–1534, 2016. https://doi.org/10.1017/S0033291716000167
51. Wong CG, Stevens MC: The Effects of Stimulant Medication on Working Memory Functional Connectivity in Attention-Deficit/Hyperactivity Disorder. Biol Psychiatry 71:458–466, 2012. https://doi.org/10.1016/j.biopsych.2011.11.011
52. Landin-Romero R, McKenna PJ, Salgado-Pineda P, Sarró S, Aguirre C, Sarri C et al.: Failure of deactivation in the default mode network: a trait marker for schizophrenia? Psychol Med 45:1315–1325, 2014. https://doi.org/10.1017/s0033291714002426